Physica Medica 138 (2025) 105186

Contents lists available at ScienceDirect

Physica Medica

journal homepage: www.elsevier.com/locate/ejmp

Original paper

Estimation liver radiomics from postmortem CT: Development of interpretable models for postmortem interval estimation

Fabio De-Giorgio [a,b,*], Davide Cusumano [a,c], Luca Vellini [a,c], Roberto Gatta [d,e], Luca Boldrini [a,f], Matteo Mancino [a,f], Michail E. Klontzas [g,h,i], Elena F. Kranioti [j], Evis Sala [a,f], Vincenzo L. Pascali [a,b]

[a] Fondazione Policlinico Universitario A. Gemelli IRCCS, Rome, Italy
[b] Department of Healthcare Surveillance and Bioethics, Section of Legal Medicine, Università Cattolica del Sacro Cuore, Rome, Italy
[c] Mater Olbia Hospital, Olbia, Italy
[d] Dipartimento di Scienze Cliniche e Mentali, Università degli Studi di Brescia, Brescia, Italy
[e] Department of Oncology, Lausanne University Hospital, Switzerland
[f] Department of Diagnostic Imaging, Oncological Radiotherapy and Hematology, Università Cattolica Sacro Cuore, Rome, Italy
[g] Department of Medical Imaging, University Hospital of Heraklion, Voutes, Heraklion 71110 Crete, Greece
[h] Department of Radiology, Medical School, University of Crete, Voutes, Heraklion 71110 Crete, Greece
[i] Advanced Hybrid Imaging Systems, Institute of Computer Science – FORTH, Voutes, Heraklion 71110 Crete, Greece
[j] Forensic Medicine Unit, Department of Forensic Sciences, Faculty of Medicine, University of Crete, Voutes, Heraklion 71110, Greece

ARTICLE INFO

Keywords:
Computed tomography
Radiomics
Post-mortem interval

ABSTRACT

Introduction: Postmortem computed tomography (PMCT) is increasingly used in forensic investigations, offering a non-invasive and objective approach to estimating the postmortem interval (PMI). This study aimed to develop and externally validate radiomic models to distinguish deaths within versus beyond 24 h, using liver radiomic features from PMCT scans..

Methods: A retrospective analysis was performed on 51 cadavers for model development and validated on 80 independent cases. In the training set, 173 PMCT scans across different PMIs were analyzed. The liver was manually segmented, and 40 radiomic features—statistical, morphological, and fractal—were extracted. Robustness to segmentation variability was assessed with autocontoured segmentations using the Intraclass Correlation Coefficient (ICC). PMI was dichotomized as $\leq$ 24 versus $>$ 24 h. Univariate analyses identified predictive features, and logistic regression models were built from significant variables. Model performance was evaluated with receiver operating characteristic (ROC) curves, with sensitivity and specificity at the optimal threshold.

Results: Four features were significantly associated with PMI, with liver skewness emerging as the most predictive ($p = 9.13 \times 10^{-4}$) and robust (ICC = 0.75). A logistic regression model based on skewness achieved an AUC of 0.75 (95 % CI: 0.65–0.86) and 100 % specificity at the optimal threshold, reliably identifying deaths beyond 24 h. Adding a second feature did not improve performance ($p = 0.54$, DeLong test). External validation confirmed specificity of the skewness model (70 % at the optimal threshold).

Conclusion: Liver skewness extracted from PMCT shows potential as a biomarker for identifying deaths beyond 24 h, with performance confirmed on an independent cohort.

1. Introduction

The estimation of the postmortem interval (PMI) is a critical component in forensic investigations, providing essential information for both legal and medical purposes. Traditionally, PMI estimation has been based on macroscopic examination, histological findings, and biochemical analyses [1].

However, these methods are often influenced by subjectivity and

* Corresponding author at: Department of Healthcare Surveillance and Bioethics, Section of Legal Medicine, Università Cattolica del S. Cuore, Largo Francesco Vito 1, 00168 Rome, Italy.
E-mail address: fabio.degiorgio@unicatt.it (F. De-Giorgio).

https://doi.org/10.1016/j.ejmp.2025.105186
Received 24 January 2025; Received in revised form 1 September 2025; Accepted 23 September 2025
Available online 28 September 2025

environmental factors, and usually the degradation of biological markers over the time can further complicate the accuracy of the measurement of this parameter [2].

The PMI estimation can in fact be complicated by the presence of multiple factors, such as the cause of death, the environmental conditions where the subject has been found (e.g., external temperature and body location), and the individual characteristics of the deceased (e.g., body mass, body temperature, age, and gender)[3,4]. To address these challenges, a variety of methods has been explored during the years, with the choice of technique largely dependent on the body condition [5]. During the early postmortem period, physical processes such as livor mortis, rigor mortis, algor mortis, and supravital reactivity are commonly used [6]. As decomposition advances, forensic entomology and skeletal muscle protein degradation may provide more reliable information[7]. In recent years, imaging techniques have become a cornerstone of death investigations, often complementing or replacing invasive autopsy procedures[8]. Among these, postmortem computed tomography (PMCT) has emerged as a preferred modality due to its accessibility, non-invasive nature, and ability to produce high-quality contrast images [9,10]. PMCT provides valuable insights into postmortem changes across various organs, as the liver, the brain or the eyes. Recently it has been reported that the liver undergoes significant postmortem modifications visible on PMCT, such as the accumulation of intrahepatic gas, which typically appears in the portal veins 12–64 h after death and later extends to the hepatic veins [11].

In this context the idea of quantitatively analysing such images offers a unique opportunity to obtain reliable PMI estimation through the characterisation of the postmortem changes occurred in the liver and visible on PMCT. Radiomics is a recent approach born to extract high-dimensional data from medical images, so enabling the identification of subtle changes in tissue structure and composition [12,13].

Despite the promising data obtainable through the use of PMCT, its application to PMI estimation remains largely unexplored, mainly due to the lack of large, standardised dataset, where PMCT of cases acquired at different and known time points after the death are available.

This study sought to address this limitation by applying radiomic analysis to liver PMCT images of a comprehensive cohort of patients acquired with well-known postmortem interval and then evaluated using an external independent cohort. Quantitative features extracted from the liver were used to develop predictive models capable of distinguishing between deaths occurring within or beyond 24 h postmortem. A key focus of this study was ensuring model interpretability, which is essential in modern radiomic approaches. Understanding the mechanisms underlying model predictions is critical not only for fostering trust among clinicians but also for enabling the effective translation of these models into practical forensic and clinical applications.

2. Materials and methods

2.1. Subjects

This retrospective study included cadavers referred to the Forensic Medicine Institute of Università Cattolica del Sacro Cuore (UCSC), Rome, between May 2021 and May 2023, and to the University Hospital of Heraklion, Crete, between August 2016 and November 2021.

The model was trained on a total of 51 subjects, with a mean age at death of 59.3 years (range: 15–86 years). Of these, 9 were female and 42 were male. Inclusion criteria consisted of a verified time of death (confirmed by witnesses) and an age above 15 years. Exclusion criteria encompassed clinically and/or radiologically significant liver pathologies or traumatic liver injuries.

Following the same inclusion and exclusion criteria applied to the training cohort, a total of 80 subjects were enrolled for external validation. The cohort had a mean age of 45.9 years (standard deviation: 23.8 years), with males representing 76 % of the population.

The study received the approval of the Institutional Research Ethics Committee. All the bodies were transported to the Institute within maximum six hours of death. Upon arrival, the bodies were undressed, placed supine on the CT table in the scanning room with arms positioned alongside the torso, and placed in standard forensic body bags. The cadavers remained in this position throughout the entire procedure, conducted in a controlled environment maintained at a temperature of 18–20 °C and relative humidity of 49 %. Each case underwent a variable number of sequential CT scans prior to autopsy.

As for the training set, all CT examinations were acquired using a Somatom Scope 16-slice CT scanner (Siemens Healthineers, Italy) and alternated between two acquisition protocols. Protocol 1 employed 130 kV voltage, 71 mA tube current, 1.5 mm slice thickness, and H31S head-district kernel reconstruction. Protocol 2 utilized 130 kV voltage, 90 mA tube current, 1.5-mm slice thickness, and H75 kernel reconstruction. For all scans the full body was acquired, from the vertex of the skull to beyond the feet, without the use of contrast agent. All scans were reviewed by a senior radiologist to ensure reliability and image quality; scans with artifacts were repeated as necessary. Following CT evaluation, all cadavers underwent autopsy, complemented by standard histological and toxicological analyses. The entire investigative process (postmortem CT examinations, autopsies, and ancillary analyses) was conducted with authorization from the Judicial Authority.

As for the external test set, whole-body PMCT examinations were performed using a 128-slice Revolution Gemstone Spectral Imaging CT scanner (General Electric Medical Systems, USA). Acquisition parameters were set at 120 kV tube voltage, 120 mA tube current, 0.625 mm slice thickness, and a reconstruction matrix of 512 × 512 pixels. The same procedures applied in the training set regarding autopsy and ancillary analyses were consistently adopted for the external validation cohort.

2.2. Radiomic analysis

CT images were imported into the 3D Slicer platform (v5.4.0) for liver delineation, which was performed manually by a radiologist. The resulting DICOM files and RT structure sets, containing both the images and contours, were then exported and processed using Moddicom, an open-source, IBSI-compliant radiomic analysis platform developed in R (v4.3.0) [14,15].

Radiomic features were extracted from two feature families: morphological and statistical. Second-order features were excluded to prioritize model interpretability, aligning with the study's objective. Morphological features were derived directly from the delineated contours, while an image pre-processing was evaluated for first-order features to address variability from differing image acquisition protocols. This pre-processing pipeline included computing the 1st and 99th percentiles of the grey-level histogram within the region of interest (ROI) and normalizing grey levels to these percentile values. Additionally, fractal features were calculated following methods outlined by Cusumano et al in previous radiomic studies carried out on rectal cancer patients [16–18].

For each CT image, a total of 40 features were extracted: 21 statistical, 14 morphological, and 5 fractal features. Due to the considerable variation in acquisition times across cases, the PMI was divided into 12-hour intervals. Radiomic features from CT scans acquired within the same time interval were averaged to minimize variability. Consequently, for each patient, radiomic features representing the liver were available at 12-hour intervals postmortem.

A binary outcome was assigned to each CT acquisition: 0 for acquisitions from patients who had died within 24 h and 1 for acquisitions from patients who had died more than 24 h prior.

To assess the distribution of radiomic feature values in relation to the binary outcome, the Shapiro-Wilk test was applied to evaluate normality. For univariate analysis, the ability of each feature to predict the binary outcome was determined using Wilcoxon Mann-Whitney

(WMW) for non-normally distributed dat, *t*-test for normally distributed data [19,20]. A Benjamini-Hochberg (BH) correction was applied to adjust for multiple comparisons [21].

An additional contour set was generated using an auto-contouring software (Total Segmentator) to assess the robustness of the radiomic features that were significant in the univariate analysis with respect to contour variability [22]. The Intraclass Correlation Coefficient (ICC) was calculated using a two-way random-effects model with absolute agreement and single measures, comparing the features extracted from the two contour sets. Features with an ICC greater than 0.7 were considered robust to contour variability [23].

A logistic regression model was constructed using the most significant radiomic feature identified through univariate analysis. Its predictive performance was assessed via the area under the receiver operating characteristic (ROC) curve (AUC) [24,25]. Confidence intervals for the ROC curves were calculated using bootstrap resampling (2000 iterations). The optimal discriminative threshold was determined by maximizing the Youden index, with sensitivity and specificity computed for this threshold. The whole pipeline was reported in Fig. 1 as scheme.

To explore potential two-variable models, a cross-correlation matrix was generated, combining all significant features from the univariate analysis [22]. The ROC curve for the two-variables model was calculated using the same methodology as the single-variable one.

The robustness of both predictive models was evaluated using a 10-fold cross-validation repeated 300 times. The two ROC curves were then compared using DeLong test, which allowed us to identify the best-performing model to be subjected to external validation.

Applying this logistic model, the probability of PMI occurring before or after 24 h was calculated for each case in the external test set: predictions were then dichotomized according to the optimal threshold derived from the training set, and values of sensitivity, specificity, and overall accuracy were computed to evaluate the predictive performance of the model on the external cohort.

3. Results

3.1. Dataset Overview and univariate analysis

Each subject belonging to the training set underwent an average of 3.4 CT scans (range: 1–16; SD = 3.5), with acquisitions performed at varying postmortem intervals. The mean PMI across all acquisitions was 31.9 h (range: 3.7–219.3 h; SD = 3.9). The first scan for each subject was conducted at an average PMI of 16.6 h (range: 3.7–164.2 h; SD = 33.3).

The total training dataset included 173 PMCT acquisitions. Following averaging across 12-hours time intervals to minimize variability, the dataset was reduced to 80 acquisitions. Of these, 31 scans (38.8 %) were performed within 24 h of death, providing a balanced distribution for subsequent analyses.

For the test set, a total of 80 cases were included, each represented by a single CT scan: among these, 25 % (20 cases) corresponded to deaths occurring within 24 h.

Univariate analysis identified four radiomic features as significant predictors of PMI, with adjusted p-values below 0.05 after applying the Benjamini-Hochberg correction for multiple comparisons. The most significant feature was the skewness of the grey-level histogram, with a p-value of 9.13×10^{-4}.

Table 1 presents the complete list of significant features identified at the univariate analysis together with the results of the ICC: all these features belonging to statistical family and were extracted by the raw PMCT images.

Table 1
List of the significant features at the univariate analysis in predicting patients died after 24 h, together with the results of repeatability analysis express in terms of ICC.

Radiomic feature	Adjusted p-value	ICC (95 % Confidence Interval)
Skewness	0.0009	0.75 (0.68–0.81)
Kurtosis	0.0031	0.63 (0.53–0.71)
Entropy	0.0313	0.79 (0.70–0.85)
Minimum value	0.0449	0.82 (0.76–0.86)

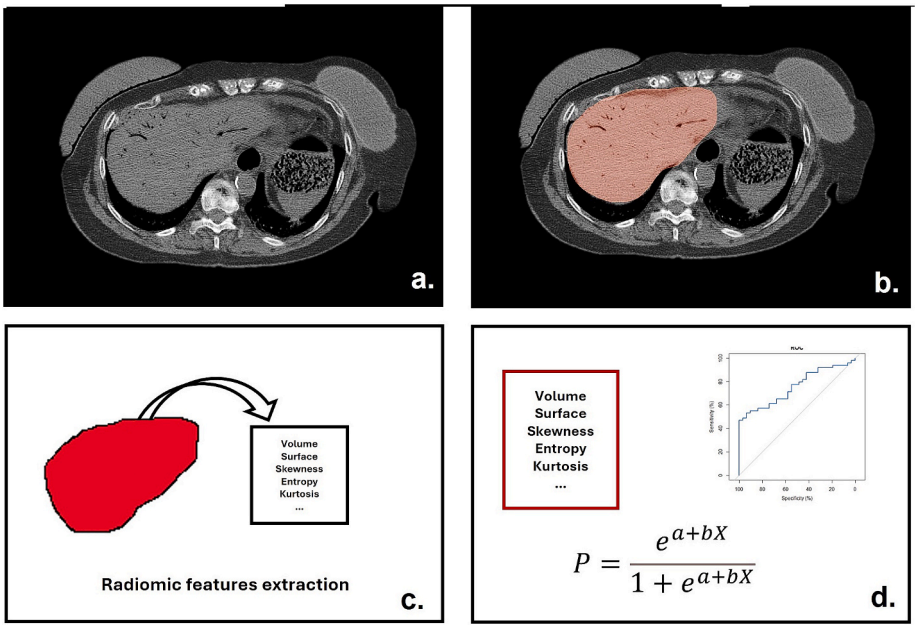

Fig. 1. Pipeline reporting the workflow followed for the methodology of the study: image collection (a), liver segmentation (b), features extraction (c) and model elaboration (d).

3.2. Single-variable logistic regression model

The skewness was selected to construct the initial logistic regression model, based on which the probability P of the cadaver having died within 24 h was calculated based on the skewness value X:

$$P = \frac{e^{a+bX}}{1 + e^{a+bX}}$$

where a = − 0.581 ± 0.342 and b = − 0.647 ± 0.198. Fig. 2 displays the receiver operating characteristic (ROC) curve for this model, with confidence intervals represented by dashed lines.

The model achieved an area under the ROC curve (AUC) of 0.75 (95 % CI: 0.65–0.86), with 0.74 ± 0.08 at the cross-validation analysis. At the optimal discriminative threshold (74.9 %), the model demonstrated a specificity of 100 %, making it highly reliable for identifying deaths occurring more than 24 h prior. However, the model's sensitivity was only 45 %, underscoring its limitations for predicting deaths within 24 h.

3.3. Two-Variable logistic regression model

A cross-correlation matrix (Fig. 3) was calculated to assess relationships among the significant features identified in the univariate analysis.

The two features with the lowest correlation (R = 0.35), minimum grey-level value and kurtosis, were selected to construct a two-variables logistic regression model. This model achieved an AUC of 0.75 (95 % CI: 0.66–0.86), with a specificity of 100 % and a sensitivity of 47 % at the optimal discriminative threshold: figure 4 reports its ROC curve. Cross-validation reported an average AUC of 0.75 ± 0.07.

The DeLong test comparing the ROC curves of the two models found no statistically significant difference (p = 0.54).

The best model (single variable) was then subjected to external validation. At the best discriminative threshold, the model reports an accuracy of 57 %, confirming an high value of specificity (70 %) and limited performance in sensitivity (20 %) (Fig. 4).

4. Discussion

This study underscores the potential of liver radiomic features derived from PMCT for PMI estimation: while radiomic and fractal analyses in PMCT have been previously explored, most existing studies are limited by small sample sizes, reducing their statistical significance [4,26–28].

The largest study to date, conducted by Klontzas et al., utilized a machine learning model based on 97 PMCTs and combined 10 radiomic features from the liver and pancreas to predict deaths occurring within 12 h, achieving an AUC of 0.75 [29].

The strength of the present study lies in achieving comparable predictive performance (AUC = 0.75) using a single, interpretable radiomic feature extracted solely from the liver. Although the PMI thresholds differ between the studies (12 h in [29] versus 24 h in this work), the development of a single-variable, biologically interpretable model enhances its applicability in forensic practice compared to black-box approaches.

The proposed model relies on the skewness of the grey-level histogram, a feature that quantifies a well-documented postmortem phenomenon: the accumulation of intrahepatic gas. This process, as described by Takahashi and others [11,30]. alters the distribution of grey levels within the liver, resulting in a characteristic shift in

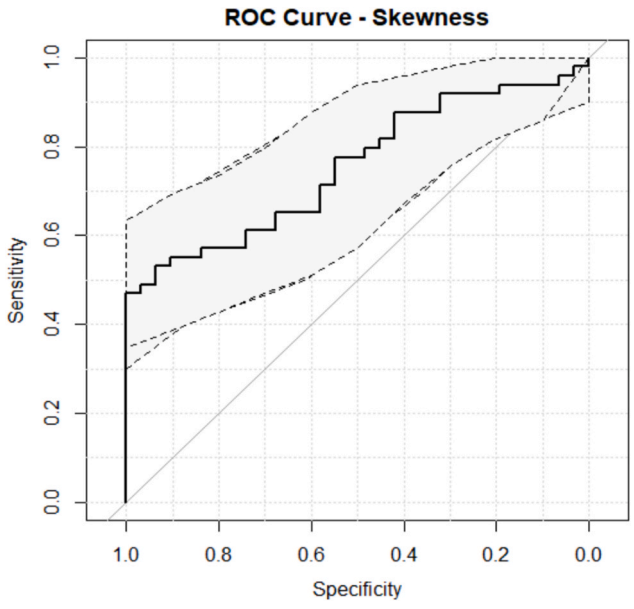

Fig. 2. ROC curve of the logistic regression model based on the skewness.

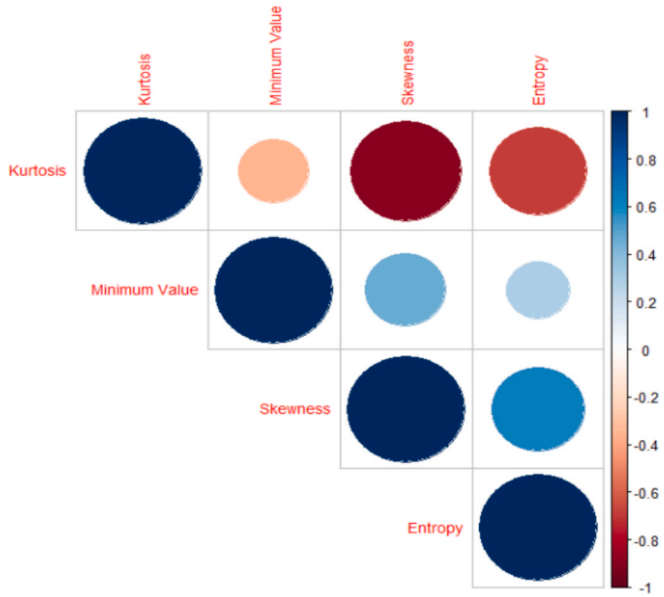

Fig. 3. Cross-correlation matrix among significant features.

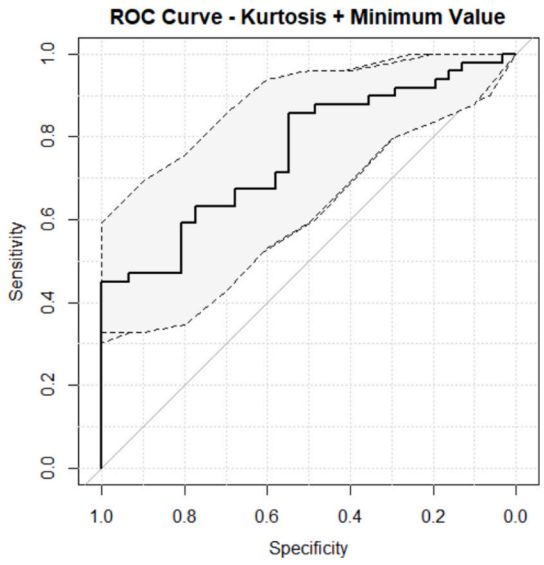

Fig. 4. ROC curve of the logistic regression model with two variables.

histogram asymmetry. The simplicity and interpretability of the skewness-based model provide a significant advantage, enabling reliable and straightforward predictions of PMI with direct applicability in forensic investigations.

Fig. 5 illustrates this phenomenon in a subject scanned at 13 h and 33 h postmortem: the increased gas content shifts the liver grey level histogram towards lower values, with the region in proximity of −1000 intensifying, leading to a more pronounced negative skewness.

When skewness value falls below −2.8, the model reliably identifies deaths occurring more than 24 h prior, reporting a 100 % of specificity across this dataset. On the other hand, when the skewness value exceeded −2.8, the model is unable to predict PMI accurately.

The results of the DeLong test further validated the simplicity and robustness of this approach, showing no significant difference in performance between the single and two-features model. This suggests that skewness alone captures the majority of the discriminatory power, underscoring the importance of selecting radiomic features with strong biological correlation and minimal redundancy, as also reported in other radiomic approaches focused on other scopes [31,32].

Another strength of this study is the inclusion of an external validation cohort, which confirmed the high specificity initially observed in the training set (100 %), with consistent results also in the test set (70 %) despite differences in acquisition protocols and the use of a different center. To the best of our knowledge, this represents one of the first experience in the forensic radiomic applications including external validation.

Considering also the external validation, this model, if further validated across additional centers, could be used in the future to identify corpses whose death occurred more than 24 h earlier. The model can only be applied in one direction: if the skewness value in the liver is below −2.8, then there is a very high probability (70–100 %) that the person has been dead for more than 24 h. However, if the skewness value is above this threshold, no reliable prediction can be made regarding the PMI.

Clearly, this work should be considered a pilot study: the next step will be to expand it into a multicenter project with harmonized postmortem acquisition times and acquisition protocols. Nonetheless, the consistently high specificity suggests that the calculation of liver skewness may represent a reliable and contour-robust parameter to identify cadavers with a postmortem interval longer than 24 h.

However, the binary nature of the model restricts its utility in cases requiring finer temporal resolution: developing continuous models capable of estimating PMI with higher granularity remains a critical next step and an area of active research.

Expanding the scope of radiomic analysis beyond the liver may also improve predictive accuracy, as organs such as the brain or eyes could offer complementary insights. For example, a recent study analysed postmortem changes in the eye, including lens dislocation and intraocular pressure variations, identifying time-dependent processes that could be leveraged for PMI estimation [33]. While this study was not radiomic in nature, its findings highlight the potential of the eye as a target for future radiomic analyses, paving the way towards the use of multi-organ radiomic approaches to improve overall model performance.

5. Conclusions

In conclusion, this study demonstrates the potential of a skewness-based model for PMI estimation, offering a robust, interpretable approach with excellent specificity for identifying deaths beyond 24 h. While additional research is needed to address current limitations, these findings pave the way for the broader application of radiomics in forensic medicine, providing an objective, non-invasive alternative to traditional methods.

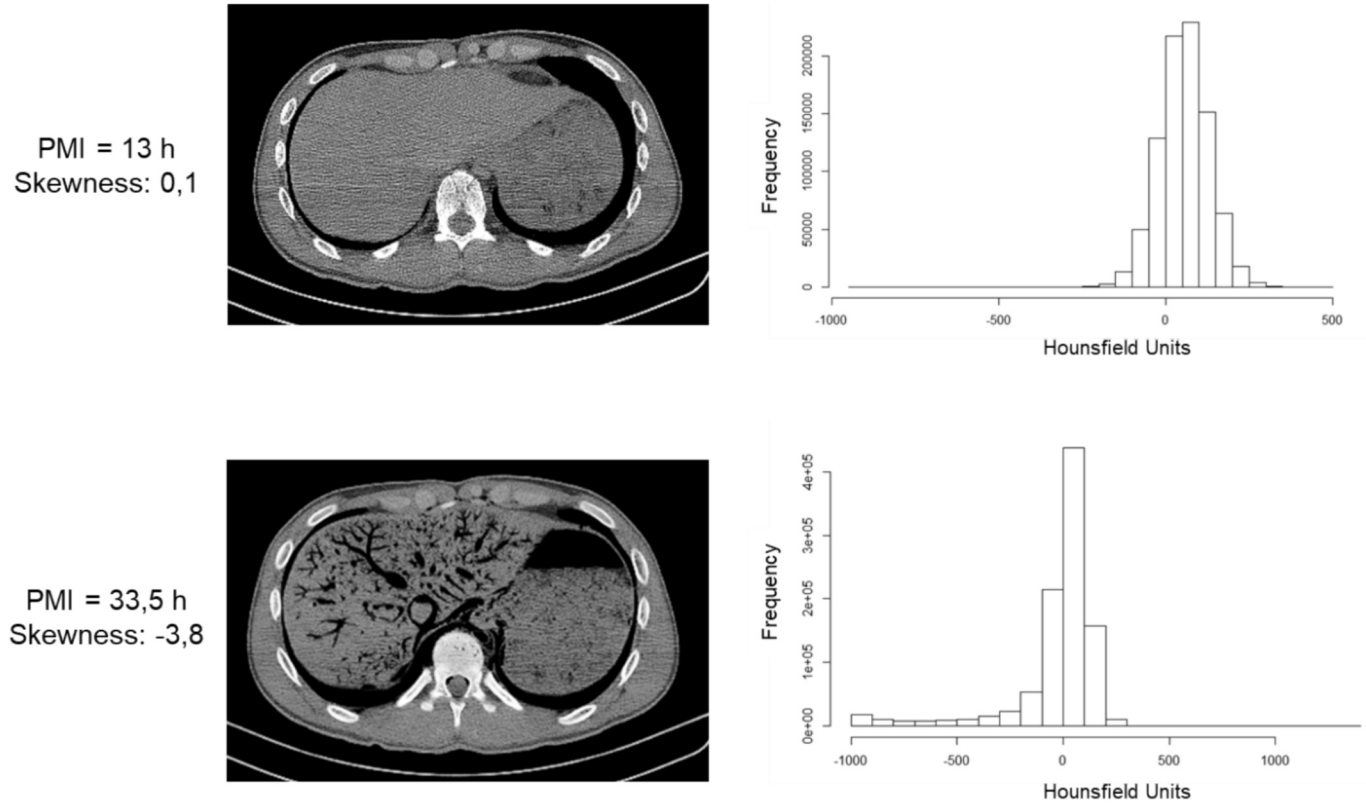

Fig. 5. Comparison of two PMCT scans acquired from the same patient at different PMIs. As time progresses, the formation of air bubbles results in significant alterations in the liver's grey-level histogram, highlighting changes in tissue composition.

8. Consent to participate

Not needed.

9. Consent to publish

Not needed.

Ethics approval

The study was approved by the Institutional Research Ethics Committee (ID 3862). Consent to participate and consent for publication: Not needed.

Funding

This work has been supported by Fondi di Ateneo, Linea D1—Università Cattolica del Sacro Cuore, grant no. R4124500826 to F. D.G.

Declaration of competing interest

The authors declare that they have no known competing financial interests or personal relationships that could have appeared to influence the work reported in this paper.

References

[1] Madea B. Estimating time of death from measurement of the electrical excitability of skeletal muscle. J Forensic Sci Soc 1992;32:117–29. https://doi.org/10.1016/S0015-7368(92)73061-8.
[2] Henssge C, Madea B. Estimation of the time since death in the early post-mortem period. Forensic Sci Int 2004;144:167–75. https://doi.org/10.1016/j.forsciint.2004.04.051.
[3] Madea B. Methods for determining time of death. Forensic Sci Med Pathol 2016;12:451–85. https://doi.org/10.1007/s12024-016-9776-y.
[4] Henssge C. Death time estimation in case work. I. the rectal temperature time of death nomogram. Forensic Sci Int 1988;38:209–36. https://doi.org/10.1016/0379-0738(88)90168-5.
[5] Maile AE, Inoue CG, Barksdale LE, Carter DO. Toward a universal equation to estimate postmortem interval. Forensic Sci Int 2017;272:150–3. https://doi.org/10.1016/j.forsciint.2017.01.013.
[6] Postmortem Change - an overview | ScienceDirect Topics. https://www.sciencedirect.com/topics/pharmacology-toxicology-and-pharmaceutical-science/postmortem-change. Accessed 26 Nov 2024.
[7] Zhou C, Byard RW. Factors and processes causing accelerated decomposition in human cadavers – an overview. J Forensic Leg Med 2011;18:6–9. https://doi.org/10.1016/j.jflm.2010.10.003.
[8] Andrews SW. Postmortem changes as documented in postmortem computed tomography scans. Acad Forensic Pathol 2016;6:63–76. https://doi.org/10.23907/2016.006.
[9] De-Giorgio F, Boldrini L. Advanced forensic bioimaging analysis: the radiomics perspective. Forensic Sci Int: Rep 2021;4:100247. https://doi.org/10.1016/j.fsir.2021.100247.
[10] De-Giorgio F, Guerreri M, Gatta R, et al. Exploring radiomic features of lateral cerebral ventricles in postmortem CT for postmortem interval estimation. Int J Leg Med 2024. https://doi.org/10.1007/s00414-024-03396-9.
[11] Okumura M, Usumoto Y, Tsuji A, et al. Analysis of postmortem changes in internal organs and gases using computed tomography data. Leg Med (Tokyo) 2017;25:11–5. https://doi.org/10.1016/j.legalmed.2016.12.011.
[12] Lambin P, Rios-Velazquez E, Leijenaar R, et al. Radiomics: extracting more information from medical images using advanced feature analysis. Eur J Cancer 2012;48:441–6. https://doi.org/10.1016/j.ejca.2011.11.036.
[13] Lambin P, Leijenaar RTH, Deist TM, et al. Radiomics: the bridge between medical imaging and personalized medicine. Nat Rev Clin Oncol 2017;14:749–62. https://doi.org/10.1038/nrclinonc.2017.141.
[14] Dinapoli N, Alitto AR, Vallati M, et al. Moddicom: a complete and easily accessible library for prognostic evaluations relying on image features. Conf Proc IEEE Eng Med Biol Soc 2015;2015:771–4. https://doi.org/10.1109/EMBC.2015.7318476.
[15] Zwanenburg A, Vallières M, Abdalah MA, et al. The image biomarker standardization initiative: standardized quantitative radiomics for high-throughput image-based phenotyping. Radiology 2020;295:328–38. https://doi.org/10.1148/radiol.2020191145.
[16] Cusumano D, Dinapoli N, Boldrini L, et al. Fractal-based radiomic approach to predict complete pathological response after chemo-radiotherapy in rectal cancer. Radiol Med 2018;123:286–95. https://doi.org/10.1007/s11547-017-0838-3.
[17] Di Dio C, Chiloiro G, Cusumano D, et al. Fractal-based radiomic approach to tailor the chemotherapy treatment in rectal cancer: a generating hypothesis study. Front Oncol 2021;11:774413. https://doi.org/10.3389/fonc.2021.774413.
[18] Cusumano D, Meijer G, Lenkowicz J, et al. A field strength independent MR radiomics model to predict pathological complete response in locally advanced rectal cancer. Radiol Med 2020. https://doi.org/10.1007/s11547-020-01266-z.
[19] Taylor J. Introduction to Error Analysis, the Study of Uncertainties in Physical Measurements, 2nd Edition; 1997.
[20] Cusumano D, Boldrini L, Yadav P, et al. Delta radiomics analysis for local control prediction in pancreatic cancer patients treated using magnetic resonance guided radiotherapy. Diagnostics 2021;11:72. https://doi.org/10.3390/diagnostics11010072.
[21] McHugh ML. Multiple comparison analysis testing in ANOVA. Biochem Med (Zagreb) 2011;21:203–9.
[22] Wasserthal J, Breit H-C, Meyer MT, et al. Total segmentator: robust segmentation of 104 anatomic structures in CT images. Radiol Artif Intell 2023;5:e230024. https://doi.org/10.1148/ryai.230024.
[23] Cusumano D, Boldrini L, Yadav P, et al. External validation of early regression index (ERITCP) as predictor of pathologic complete response in rectal cancer using magnetic resonance-guided radiation therapy. Int J Radiat Oncol Biol Phys 2020;108:1347–56. https://doi.org/10.1016/j.ijrobp.2020.07.2323.
[24] International Commissioning on Radiation Units and Measurements (2008) Receiver Operating Characteristic (ROC) Analysis in Medical Imaging. ICRU Report 79.
[25] Chan YH. Biostatistics 104: correlational analysis. Singapore Med J 2003;44:614–9.
[26] De-Giorgio F, Ciasca G, Fecondo G, et al. Estimation of the time of death by measuring the variation of lateral cerebral ventricle volume and cerebrospinal fluid radiodensity using postmortem computed tomography. Int J Leg Med 2021;135:2615–23. https://doi.org/10.1007/s00414-021-02698-6.
[27] De-Giorgio F, Ciasca G, Fecondo G, et al. Post mortem computed tomography meets radiomics: a case series on fractal analysis of post mortem changes in the brain. Int J Leg Med 2022;136:719–27. https://doi.org/10.1007/s00414-022-02801-5.
[28] Madea B, Ortmann J, Doberentz E. Estimation of the time since death-even methods with a low precision may be helpful in forensic casework. Forensic Sci Int 2019;302:109879. https://doi.org/10.1016/j.forsciint.2019.109879.
[29] Klontzas ME, Leventis D, Spanakis K, et al. Post-mortem CT radiomics for the prediction of time since death. Eur Radiol 2023;33:8387–95. https://doi.org/10.1007/s00330-023-09746-2.
[30] Takahashi N, Higuchi T, Shiotani M, et al. Intrahepatic gas at postmortem multislice computed tomography in cases of nontraumatic death. Jpn J Radiol 2009;27:264–8. https://doi.org/10.1007/s11604-009-0337-0.
[31] Cusumano D, Catucci F, Romano A, et al. Evaluation of an early regression index (ERITCP) as predictor of pathological complete response in cervical cancer: a pilot-study. Appl Sci 2020;10:8001. https://doi.org/10.3390/app10228001.
[32] Cusumano D, Russo L, Gui B, et al. Evaluation of early regression index as response predictor in cervical cancer: a retrospective study on T2 and DWI MR images. Radiother Oncol 2022;174:30–6. https://doi.org/10.1016/j.radonc.2022.07.001.
[33] Yoshimiya M, Shimbashi S, Hyodoh H. Postmortem changes in the eye on computed tomography images. Leg Med (Tokyo) 2024;70:102477. https://doi.org/10.1016/j.legalmed.2024.102477.